J. Phys. Chem. C **2008,** *112,* 17303–17310

The Effect of Water on the CO Oxidation on Ag(111) and Au(111) Surfaces: A First-Principle Study

Hai-Yan Su,[†,‡,§] **Ming-Mei Yang,**[†,‡,§] **Xin-He Bao,**[†] **and Wei-Xue Li***[,†,‡]

State Key Laboratory of Catalysis, Dalian Institute of Chemical Physics, Chinese Academy of Sciences, Dalian, 116023, China, Center for Theoretical and Computational Chemistry, Dalian Institute of Chemical Physics, Chinese Academy of Sciences, Dalian, 116023, China, and Graduate School of the Chinese Academy of Sciences, Beijing, 100039, China

Received: April 18, 2008; Revised Manuscript Received: August 22, 2008

Density functional theory has been used to study the effect of water on the molecular (O_2, O, and CO) adsorption, O_2 dissociation, and CO oxidation on the Ag(111) and Au(111) surfaces. It is found that, though CO oxidation with atomic O is facile on both surfaces with barriers less than 0.29 eV, considerable barriers for O_2 dissociation (1.03 eV for Ag(111) and 1.97 eV for Au(111)) and weak adsorption of reactants limit their overall reactivity. Our calculations show that the reactants can be stabilized by coadsorption of water via the formation of an H bond and/or the interaction mediated through the substrates. The stabilization induced by coadsorbed water affects not only adsorption of reactants but also the transition states and intermediates, which enhances overall reactivity for CO oxidation, correspondingly. H bonds facilitate the dissociation of O_2 with reduction of barrier by 0.36 eV on Ag(111). Moreover, a highly active reaction pathway for CO oxidation via molecular assistant by water with overall barrier of 0.15 eV is identified. Atomic oxygen formed may either react with adsorbed CO or react with adsorbed water to form hydroxyls, which oxidizes CO subsequently, to complete the catalytic cycle.

1. Introduction

CO oxidation on transition metal (TM) surfaces is one of the most important catalytic reactions among others, primarily for two reasons: [1−3] technologically, it is an important reaction in car-exhaust emission control, CO_2 lasers, and sensors etc. Scientifically, it is one of the simplest catalytic reactions and thus has been widely used as model system for the mechanism study of heterogeneous catalysis. So far, there are two possible mechanisms for CO oxidation on the TM surfaces proposed. The first one suggested that CO oxidation mainly consists of two elementary processes on the TM surfaces: dissociative adsorption of molecular oxygen followed by reaction between dissociated oxygen and adsorbed CO to form CO_2. Depending on the reactivity of the TMs, the rate-limiting step (RLS) for CO oxidation could be totally different.[4−30] For TMs that bind oxygen strongly (corresponding to the left of the periodic table), the rate was limited by the mobility of adsorbed O and CO and recombination reaction between reactants.[4−6] For TM surfaces that bind oxygen weakly (such as Ag and Au), the reaction rate was limited by the dissociation of O_2. In this case, CO oxidation may proceed via another mechanism, where molecular oxygen directly interact with CO forming a four-center surface complex $O_2\cdots CO$, which released CO_2 and atomic O afterward.[7−30] This mechanism was stimulating since there was no demanding activation of O_2 required before reacting with CO, and CO oxidation could proceed at low temperatures, which may have potential application for lower temperature CO removal and proton exchange membrane fuel cell (PEMFC).

CO oxidation going through by oxygen molecules on Ag has been investigated experimentally by Burghaus et al.[14−17] They measured the CO_2 production rate with a mass spectrometer, and substantial reaction has been observed upon the admission of CO via a molecular beam onto an O_2 layer under the condition well below the dissociation temperature of O_2.[16] The mechanism proposed as $CO + O_2 \rightarrow O_2\cdots CO \rightarrow CO_2 + O$ was corroborated further by Barth and Zambelli using scanning tunneling microscopy (STM) at the temperature range of 60−110 K.[18] For Au single crystals, it was found that oxygen dissociative adsorption at temperatures below 673 K was significantly hindered by a high O_2 dissociation barrier,[19] which was supported by density functional theory (DFT) calculations.[12] CO oxidation occurs readily when oxygen was provided in atomic form.[19,20] For supported Au catalysts, the mechanism for oxygen adsorption and activation remains controversial. Two mechanisms have been proposed and differ from each other on where and how molecular O_2 is activated. The first mechanism suggested that on the highly dispersed Au particles: (i) O_2 can adsorb, and (ii) adsorbed O_2 either directly dissociates or interacts with CO forming a four-center surface complex.[21−23] The second mechanism suggested that the adsorption and activation of O_2 occur either dominantly on the support or at the metal/support interface.[24−28] Mullins et al. presented experimental evidence for reaction of CO with molecularly chemisorbed oxygen on TiO_2-supported gold nanoclusters at 77 K.[29] DFT calculations showed that CO oxidation by reacting with molecular oxygen via $O_2\cdots CO$complex was found to yield energetically favorable reaction paths with a barrier of 0.46 eV for vicinal Au surfaces[12] and 0.27 eV for MgO-supported Au clusters,[13] respectively.

Haruta and co-workers found that with addition of small amount of moisture up to 200 ppm, reaction rates for CO oxidation on supported gold nanoparticles increases orders of

---

* To whom correspondence should be addressed. E-mail: wxli@dicp.ac.cn.

[†] State Key Laboratory of Catalysis, Dalian Institute of Chemical Physics.

[‡] Center for Theoretical and Computational Chemistry, Dalian Institute of Chemical Physics.

[§] Graduate School of the Chinese Academy of Sciences.

10.1021/jp803400p CCC: $40.75

magnitude.[30] The promotion of water on CO oxidation has also been reported on Pt(111).[31,32] Role of water has been speculated to assist the reaction by either activating the molecular oxygen or decomposing carbonates in CO oxidation on the Au nanoparticles.[33] Recently, Mullins, Henkelman, and co-workers studied experimentally and theoretically CO oxidation on atomic oxygen precovered Au(111) and found that the reaction rate increases significantly with exposure of water.[34,35] By the interplay between isotope experiments and DFT calculations, they showed clearly that water was involved directly in the CO oxidation. Theoretically, the effect of water on CO oxidation has been addressed by Hu and co-workers using DFT,[32] who proposed that CO oxidation on Pt(111) was facilitated by reacting with hydroxyl group from reaction of H_2O and O. They also investigated the role of water in CO oxidation on Au/TiO_2(110). They found that water can dissociate readily into OH groups, which facilitates O_2 adsorption and diffusion on TiO_2, and activity increased correspondingly.[36] Landman and co-workers[37] showed that coadsorption of H_2O and O_2 leads to formation of a complex well bound to the free and supported gold cluster due to the proton sharing between adsorbates. The O−O bond is thus activated, leading to a small activation barrier for CO oxidation (0.5 eV).

Though promotion of CO oxidation by water was appreciated, the detailed mechanism remained elusive. For example, how does adsorbed water affect the adsorption of reactants such as O, CO, and O_2? Would water molecules form separated domain or mix with the reactants? Would O_2 dissociation be changed by the presence of water? Whether CO oxidation proceeds with O_2 or atomic oxygen? How does CO oxidation proceed via the presence of water? Was water directly or indirectly as a spectator involved in the reaction and how? These questions were addressed here by a first-principle density functional theory study on Ag(111) and Au(111).

The paper is organized as follows. The calculation methods are introduced in section 2. In section 3, the results of the CO oxidation on the clean TM surfaces are reported. The effects of H_2O on the adsorption of the various reactants are discussed in section 4. Then the effect of H_2O on O_2 dissociation and CO oxidation on the TM surfaces are studied in section 5 and discussed in section 6. A brief summary is given section 7.

2. Methods

The spin-polarized DFT calculations were performed using the DACAPO package,[38] where an ultrasoft pseudopotential was used to describe the ionic cores. The Kohn−Sham one-electron valence states were expanded in a plane-wave basis set with kinetic cutoff at 340 eV. The exchange-correlation energy and potential was described by the generalized gradient functional GGA-PW91.[39,40] During iterative diagonalization of the Kohn−Sham Hamiltonian, Fermi population of the Kohn−Sham states ($k_BT = 0.1$ eV) and Pulay mixing of the resulting electronic density was used to improve the convergence, and the total energy was extrapolated to absolute zero correspondingly.

The TM surfaces were represented by a four-layer slab separated by seven equivalent layers of vacuum. The top two layers of the slab and adsorbates were relaxed up to residual forces less than 0.02 eV/Å. Supercells with periodicity (2 × 2) have been employed to simulate adsorption and reaction of various adsorbates on TMs. A Monkhorst Pack mesh with a (4 × 4 × 1) grid was used for k-point sampling in the surface Brillouin zone of the unit cells. When large (3 × 3) and (2 × 3) supercells have been used, k-point samplings were changed accordingly. Calculated equilibrium lattice constants for bulk Ag (4.14 Å) and Au (4.17 Å), consistent with the experiments measurements and previous DFT study,[41−43] were employed throughout the present paper. Calculations for the isolated gas-phase molecules were carried out in a (12.0 Å × 12.1 Å × 12.2 Å) unit cell, and the Brillouin zone was sampled with a single k point. The calculated gas-phase H_2 and O_2 bond energies are −4.56 and −5.57 eV, and the corresponding experimental values are −4.48 and −5.12 eV, respectively.[44]

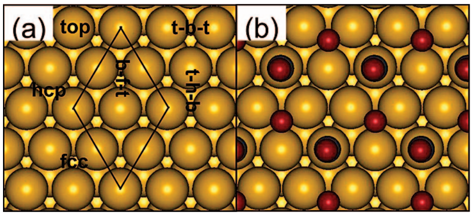

Figure 1. Top view of (a) the possible adsorption sites on surfaces and (b) CO and O coadsorption on the Ag(111) and Au(111) surfaces. The metal atoms, O atoms, and C atoms are represented by the yellow, red, and gray balls, respectively. The unit cell used is delineated.

Adsorption was allowed on the relaxed side of the slab only, with the electrostatic potential adjusted accordingly. The adsorption energy (E_{ads}) of an adsorbed atom or molecule was calculated as

$$E_{ads} = E_{total} - E_{slab} - 1/NE_{mol} \tag{1}$$

which corresponds to energy gain with respect to the adsorbates in gas phase and the metal slab. For atomic O adsorption, E_{ads} represents the average dissociative adsorption energy where $N = 2$, while for the molecule adsorption, $N = 1$. E_{total}, E_{slab}, and E_{mol} are the total energies of the optimized adsorbate−substrate system, clean surfaces, and the molecules in the gas phase, respectively. Here, a negative (positive) value represents the adsorption is exothermic (endothermic). For the coadsorption system, overall adsorption energy with respect to clean substrate E_{coads} was defined accordingly. To study lateral interaction between the adsorbates coadsorbed on the surfaces, so-called differential adsorption energy E_{ads} was defined as the energy gain with respect to the preadsorbed species.

The transition states (TS) of the reactions were searched by constraining the distance between the reactants and relaxing all the other degrees of freedom, the so-called constrained minimization technique. The incremental step was separated by less than 0.1 Å with care being taken that the pathways (potential energy surfaces) become continuous.[45]

3. CO Oxidation on Ag(111) and Au(111) Surfaces

3.1. Adsorption. As a starting point, we studied the adsorption (E_{ads}) of the reactants (CO, O_2, O, and H_2O) on Ag (111) and Au (111), as shown schematically in Figure 1a. Calculated adsorption energies and other important parameters are listed in Table 1. All molecules adsorb weakly on both surfaces, as expected from the nobleness of Ag and Au. Specifically, the calculated adsorption energies were −0.16 eV/O_2, −0.42 eV/O, −0.29 eV/CO, and −0.17 eV/H_2O on Ag (111) and −0.04 eV/O_2, 0.15 eV/O, −0.29 eV/CO, and −0.15 eV/H_2O on Au (111), respectively, which are consistent with the previous DFT calculations.[7,46] It can be found that, though the energy for CO and H_2O adsorption on Ag(111) and Au(111) is close, adsorption of O_2 and atomic O on the latter one was energetically less stable then adsorption on the previous one. Actually, the adsorptions on Au(111) are thermal neutral or even endothermic. As shown in Figure 1a, the top site, face-centered cubic (fcc) site, top−bridge−top (t-b-t), and the top site are energetically

TABLE 1: Calculated Adsorption Energy (E_{ads} in eV), Magnetic Moment (μ_m in μ_B), and Variation of Work Function ($\Delta\phi$ in eV) on the Ag(111) and Au(111) Surfaces in (2 × 2) Unit Cell

		Ag(111)			Au(111)		
adsorbates	site	E_{ads}	μ_m	$\Delta\phi$	E_{ads}	μ_m	$\Delta\phi$
CO	top	−0.29		−0.08	−0.29		−0.56
	bri	−0.21		0.32	−0.30		0.27
	fcc	−0.24		0.41	−0.25		0.37
O	fcc	−0.42		1.16	0.15		0.66
	hcp	−0.30		1.22	0.39		0.77
O_2	t-b-t	−0.16	1.29	1.29	−0.04	1.99	0.10
	b-f-t				−0.04	1.99	0.11
	b-h-t	−0.07	1.28	1.25	−0.04	1.99	0.10
H_2O	top	−0.17		−0.18	−0.15		−0.23

TABLE 2: Calculated Adsorption Energy E_{coads} and Variation of Work Function $\Delta\phi$ for Co-Adsorbed CO and O with Respect to the Clean Ag(111) and Au(111) Surfaces[a]

	E_{coads}	E_{ads}(O) (fcc)	E_{ads}(CO) (top)	ΔE	$\Delta\phi$
Ag(111)	−0.94	−0.65	−0.47	−0.23	0.58
Au(111)	−0.33	−0.44	−0.54	−0.19	−0.04

[a] E_{ads}(O) and E_{ads}(CO) are the differential adsorption energies of O and CO in coadsorption configuration, respectively. ΔE is the energy difference between E_{coads} and the sum of the separated adsorption E_{ads}(O) and E_{ads}(CO) given in Table 1. The unit is electronvolts.

favorable sites for CO, O, O_2, and H_2O adsorption on both surfaces, respectively, except for CO adsorption on Au, where CO adsorption at bridge and top sites is energetically degenerate.

The O_2 at t-b-t site carries 1.28 and 1.99 μ_B of magnetic moment (compared to 2.0 μ_B in the gas phase) on Ag(111) and Au(111). As seen from Table 1, CO (top site) and H_2O adsorption induces a reduction of the work function with respect to the clean surfaces, which indicates a net electron transfer from the adsorbates to the substrates. For CO adsorption at high coordinated hollow/bridge sites, our calculations show an opposite change of work function. The reason may come from enhanced back-donation from substrate $d_{xz,yz}$ orbitals to CO $2\pi^*$ orbitals at the high coordinate sites, contrast to top site adsorption, where donation from CO 5σ orbitals to substrate d_{zz} orbitals dominates. For O and O_2 adsorption, work function increases, and this indicates a reverse electron transfer.

Having studied individual adsorption of molecules, we considered CO and O coadsorption on the surfaces. Overall adsorption energies E_{coads} and differential adsorption energies E_{ads}(CO) and E_{ads}(O) are listed in Table 2, and the optimized structure is shown schematically in Figure 1b, where for both surfaces, CO adsorbs at the top sites and O at the fcc sites. In comparison to CO adsorption on clean surfaces with energy of −0.29 eV on Ag(111) and Au(111), calculated differential adsorption energies of CO, E_{ads}(CO), are −0.47 and −0.54 eV, respectively. A significant stabilization can clearly be seen. The stabilization can be justified further from the oxygen differential adsorption E_{ads}(O) with value of −0.65 eV (vs −0.42 eV) for Ag(111) and −0.44 eV (vs 0.15 eV) for Au(111). The overall energy gain E_{coads} for CO and O coadsorption are −0.94 and −0.33 eV for Ag(111) and Au(111), in contrast to the sum of the adsorption energies of two separated species (−0.71 and −0.14 eV), respectively. The negative value of energy difference between E_{coads} and E_{ads}(O) + E_{ads}(CO), ΔE, indicates that there is net attractive interaction between coadsorbed CO and O. Correspondingly, CO and O tend to mix with each other on both surfaces instead of formation of the separated domains.

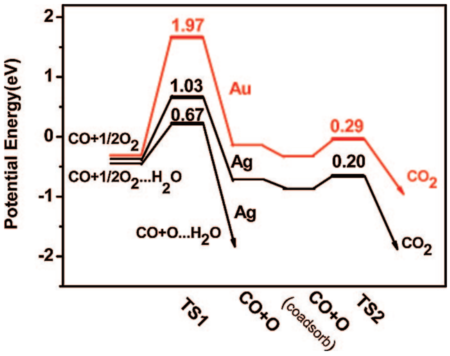

Figure 2. Potential energy surfaces for $O_2 \rightarrow 2O$ and CO + O → CO_2 reactions on Au(111) (top) and Ag(111) (middle) without and with (bottom) the presence of water. O_2 and CO (H_2O) in the gas phase have been taken as the reference state (zero of the energy axis). TS1 and TS2 represent the transition states for $O_2 \rightarrow 2O$ and CO + O → CO_2 respectively. The O_2 dissociation barrier is given by per O_2 molecule.

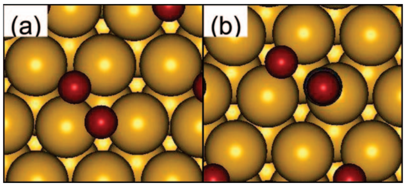

Figure 3. Schematic structures at transition states for O_2 dissociation (a) and the reaction between CO and dissociated atomic O (b).

The mechanism of the stabilization found is discussed here. On the basis of Blyholder theory,[47] the bonding of CO with Ag or Au can be described in terms of electron donation from the molecular 5σ orbital to the metal and back-donation from the metal to the empty $2\pi^*$orbital. As seen from the reduction of the work function induced by CO (top) adsorption (Table 1), adsorbed CO acts as an electron donator, while adsorbed O as an electron acceptor as seen from the increase of the work function for separated adsorption. When both molecules adsorb on the surfaces, donated electrons from CO facilitate the electron transfer from the substrate to coadsorbed O, and stabilize the system. The substrate mediated charge transfers can be corroborated from the variation of the work function for coadsorption structures (Table 2), which are roughly a sum of variation of work function from two separated species (Table 1). In comparison to the clean surface, variation of the work function of the coadsorption system increases by 0.58 eV on Ag(111) but slightly decreases by 0.04 eV on Au(111).

3.2. O_2 Dissociation and CO Oxidation. We first studied O_2 dissociation on Ag(111) and Au(111) surfaces. As seen from Figure 3a, at the transition states (TS), one O atom is located at the fcc hollow sites and remained O at the bridge sites. In comparison to the bond length of adsorbed O_2 (1.30 Å for Ag(111) and 1.24 Å for Au(111)), O_2 at TS is elongated by 0.61 Å for Ag(111) and 0.62 Å for Au(111), a typical late TS. From the potential energy surfaces shown in Figure 2, it can be seen that the E_{act} for O_2 dissociation (TS1) is 1.03 eV on Ag(111) and 1.97 eV on Au(111), which are significantly higher than corresponding energies of adsorbed O_2 (−0.16 and −0.04 eV), respectively. These results are consistent with experiments, where low O_2 dissociative sticking coefficients were found on both Ag(111) and Au(111) surfaces.[48,49]

We then investigated the reaction pathways between CO and dissociated atomic O on Ag(111) and Au(111). The transition states for the CO + O reaction on Ag(111) and Au(111) are shown in Figure 3b: O at bridge site and CO off a metal atom,

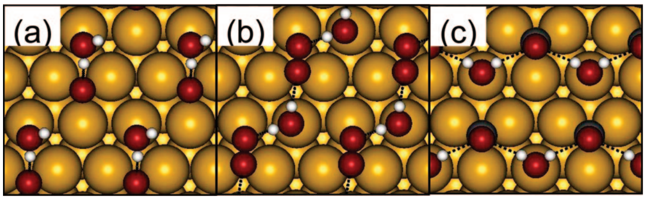

Figure 4. Schematic structures of the coadsorbed H_2O and O (a), H_2O and O_2 (b), and H_2O and CO (c) on Ag(111) and Au(111). The metal atoms, O atoms, C atoms, and H atoms are represented by the yellow, red, gray, and white balls, respectively.

tilted away from the O atom. The calculated reaction barriers are 0.20 eV for Ag(111) and 0.29 eV for Au(111) (Figure 2, TS2), which are significantly lower than other reactive TM surfaces, for instance, 1.17 eV/Rh(111), 0.79 eV/Pt(111), 1.29 eV/Ir(111), and 0.91 eV/Pd(111),[6] because of the weak interaction between adsorbates and substrates making recombination reactions less demanding. From these calculations, it is clear that, though CO oxidation with atomic O is facile on Ag(111) and Au(111), a significantly high barrier for O_2 dissociation on both surfaces make them less active for CO oxidation.

4. Effect of Water on Molecules Adsorption

To study the possible effects of water on the reactivity of CO oxidation, we describe here the coadsorption of water and atomic O on both surfaces first. Optimized structures are shown schematically in Figure 4a, where O adsorbs at the fcc sites and H_2O adsorbs at the top sites. In this configuration, the differential adsorption energy of atomic O $E_{ads}(O)$ were calculated to be -1.17 eV for Ag(111) and -0.38 eV for Au(111) (Table 3), respectively. In comparison to adsorption energy of oxygen without the presence of water (-0.42 eV for Ag(111) and 0.15 eV for Au(111) in Table 1), significant stabilization is readily seen, which can be found for H_2O too. The coadsorption energy E_{coads} for O and H_2O coadsorption are -1.20 eV for Ag(111) and -0.45 eV for Au(111), which are lower than the sum of the individual adsorption energies, -0.59 eV for Ag(111) and 0.00 eV for Au(111), respectively.

From Figure 4, it can be found that the structures of the coadsorption on Ag(111) and Au(111) surfaces are alike. Water molecules were displaced from the top sites toward atomic oxygen nearby driven by the formation of the H bonds between water and atomic oxygen. The distances between atomic O and H atom of H_2O are considerably larger on Au(111) (1.90 Å) than those of Ag(111) (1.66 Å), partially due to the larger lattice constant of Au. The large separation between atomic O and H of H_2O on Au(111) makes the contribution from the H bonds modest. The energy gain for the coadsorption was calculated to be $\Delta E = -0.45$ eV. For Ag(111), the energy gain due to the coadsorption ($\Delta E = -0.61$ eV) is significant. Though larger energy gain on Ag(111) can be attributed to the stronger H bonds formed than Au, the value remains considerably higher than the H bonds, whose strength falls typically in range of $\sim 0.2-0.3$ eV.[50] We propose here that there is the additional energy gain from the interaction mediated through the substrates. To illustrate this, we note that water adsorption induces a reduction of work function by -0.17 eV for Ag(111) and -0.15 eV for Au(111), which indicates a net electron transfer from adsorbed H_2O to the substrates. On the other hand, adsorbed oxygen is an electron acceptor. Thus, donated electrons from water to the substrates facilitate the electron transferring from substrates to adsorbed O. Adsorbed atomic O and/or waters are stabilized correspondingly, as found in above for coadsorbption of CO and O. Formation of the H bonds and the interactions mediated through the substrate indicate that there is a strong lateral interaction between water and atomic oxygen on Ag and Au surfaces.

Similar to the coadsorption of O and H_2O, we found that coadsorbed O_2 and H_2O formed a one-dimensional (1D) zigzag chain linked by the H bonds through each O atom in O_2 connected to H atoms in H_2O molecules nearby (Figure 4b). We note that in this configuration, O_2 is displaced from favorable t-b-t site to b-h-t site to maximum H bonding. Furthermore, the coadsorption pattern was found to be energetically favorable than the sum of the separated adsorptions, as seen from negative value of ΔE given in Table 4. Compared to the energy gain due to coadsorption on Au(111)($\Delta E = -0.11$ eV), the energy gain on Ag(111) with a value of $\Delta E = -0.54$ eV was again larger. The stabilization can be found further from corresponding differential adsorption energy $E_{ads}(O_2)$ and $E_{ads}(H_2O)$ listed in Table 4, where adsorption energies for separated adsorption are given in the bracket for comparison. For coadsorbed O_2 on Au(111), its bond length (1.26 Å) and magnetic moment (1.73 μ_B) remains intact with respect to the adsorption without the presence of the water (1.24 Å and 1.99 μ_B), which is in line with the modest energy gain from the coadsorption with water. Meanwhile the distance between O atoms in O_2 and H in H_2O is considerable (1.94 Å), which excludes significant contribution from possible H bonding between adsorbates. The energy gain for the coadsorption is therefore mainly from the interactions mediated through the substrates. For Ag(111), the contribution of H bonding, justified from the typical bond length between H of H_2O and O1 of O_2 (1.67Å), becomes pronounced. Accordingly, adsorbed O_2 was elongated from 1.31 to 1.41 Å and lead to zero magnetic moment.

H_2O and CO coadsorption on Ag(111) and Au(111) surfaces were studied, and energetics and main structures parameters are listed in Table 5 and shown schematically in Figure 4c. On both surfaces, it was found that CO prefers to adsorb at the hollow sites and H_2O to adsorb at the top sites. This configuration is energetically favorable than CO adsorption at the top sites, possibly because of larger steric repulsion in latter one. The overall energy gain from CO and H_2O coadsorption was however modest for both surfaces, compared to coadsorption between O/O_2 and H_2O discussed in above.

The calculations done so far showed that it is energetically favorable for reactants such as O/O_2 coadsorption with water molecules via the formation of H bonds and/or the interactions mediated through the substrates. Adsorbed water molecules could however form two-dimensional networks linked by H bonds, as found in various TM surfaces.[51,52] It is therefore interesting to know whether introduced water molecules would form separated domains or mix with coadsorbed O/O_2. Which will be formed depends sensitively on the detail energetic balances between these two adsorption patterns. To study this, we calculated the structures in a $(\sqrt{3} \times \sqrt{3})R30°$ unit cell with two water molecules inside to form cyclic hexagonal ring structures, typical structures found in refs 49 and 50. In this structure (Figure 5), there is a hydroxyl group in every second H_2O molecules not participating in H bond network, which binds to the surface either by pointing upward to the vacuum (so-called H-up configuration, panel a), or downward to the surfaces (H-down configuration, panel b). Compared to the water bilayer structures found on other TM surfaces with interlayer spacing between adjacent O layers for example 0.42 Å for Ru(0001),[50] calculated interlayer spacing were 0.09 Å and 0.07 Å for Ag(111) and Au(111), respectively. The smaller spacing be-

TABLE 3: Calculated Adsorption Energy E_{coads} and Variation of Work Function $\Delta\phi$ for Co-Adsorbed H_2O (top) and O (fcc) with Respect to the Clean Ag(111) and Au(111) Surfaces[a]

	E_{coads}	E_{ads}(O)(fcc)	$E_{ads}(H_2O)$(top)	ΔE	$\Delta\phi$	d(O−H···O)
Ag(111)	−1.20	−1.17(−0.42)	−0.76(−0.17)	−0.61	0.38	1.66
Au(111)	−0.45	−0.38(0.15)	−0.50(−0.15)	−0.45	−0.05	1.90

[a] E_{ads} (O) and $E_{ads}(H_2O)$ are the differential adsorption energies of O and H_2O in the coadsorption configuration, respectively. ΔE is energy difference between E_{coads} and the sum of the separated adsorption E_{ads}(O) and $E_{ads}(H_2O)$ given in brackets and Table 1. *d*(O−H···O) is the bond length between atomic O and H in H_2O. The unit of length is angstroms and of energy is electronvolts.

TABLE 4: Calculated Adsorption Energy E_{coads} and Variation of Work Function $\Delta\phi$ for Co-adsorbed H_2O (top) and O_2 (b-h-t) with Respect to the Clean Ag(111) and Au(111) Surfaces. $E_{ads}(O_2)$ and $E_{ads}(H_2O)$ Are the Differential Adsorption Energies of O_2 and H_2O in Coadsorption Configuration, Respectively[a]

	E_{coads}	$E_{ads}(O_2)$ (b-h-t)	$E_{ads}(H_2O)$ (top)	ΔE	$\mu_m(O_2)$	$\Delta\phi$
Ag(111)	−0.78	−0.75 (−0.07)	−0.86 (−0.17)	−0.54	0.0 (1.28)	1.60
Au(111)	−0.30	−0.23 (−0.04)	−0.29 (−0.15)	−0.11	1.73 (1.99)	0.03

	d(O1−O2)	*d*(O−H···O1)	*d*(O−H···O2)
Ag(111)	1.41 (1.31)	1.67	2.13
Au(111)	1.26 (1.24)	1.94	1.95

[a] ΔE is the energy difference between E_{coads} and the sum of the separated adsorption $E_{ads}(O_2)$ (b-h-t) and $E_{ads}(H_2O)$ given in brackets. *d*(O1−O2), *d*(O−H···O1), and *d*(O−H···O2) are the bond length between two O atoms in O_2 and O1/O2 and H in H_2O, respectively. The unit of length is angstroms and of energy is electronvolts.

TABLE 5: Calculated Adsorption Energy E_{coads} and Variation of Work Function $\Delta\phi$ for Co-Adsorbed H_2O (top) and CO (fcc) with Respect to the Clean Ag(111) and Au(111) Surfaces[a]

	E_{coads}	E_{ads}(CO)(fcc)	$E_{ads}(H_2O)$(top)	ΔE	$\Delta\phi$	d(O−H···O)
Ag(111)	−0.51	−0.36(−0.24)	−0.29(−0.17)	−0.10	−0.31	2.35
Au(111)	−0.58	−0.46(−0.25)	−0.26(−0.15)	−0.18	−0.38	2.44

[a] E_{ads}(CO) and $E_{ads}(H_2O)$ are the differential adsorption energies of CO and H_2O in coadsorption configuration, respectively. ΔE is the energy difference between E_{coads} and the sum of the separated adsorption E_{ads}(CO) (fcc) and $E_{ads}(H_2O)$ given in brackets and Table 1. *d*(O−H···O) are the bond length between O in CO and H in H_2O. The unit of length is angstroms and of energy is electronvolts.

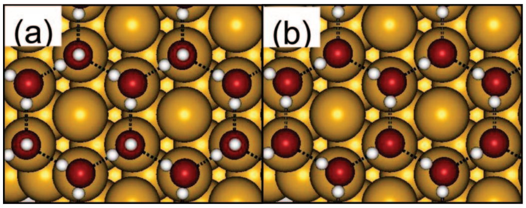

Figure 5. Schematic structures of H_2O bilayers in a $(\sqrt{3} \times \sqrt{3})R30°$ unit cell for H-up (a) and H-down (b) configurations on the Ag(111) and Au(111) surfaces.

tween O bilayers may come from large in-plane lattice constants of Ag (2.92 Å) and Au (2.96 Å) than for instance 2.72 Å for Ru(0001). In comparison to adsorbed water monomer, energy gain due to the formation of 2D H-bond network is 0.69 eV/H_2O and 0.71 eV/H_2O for Ag(111) and Au(111), respectively. We note that the energy gain by coadsorption of O/O_2 and H_2O was at best 0.61 and 0.45 eV for O and H_2O coadsorption on Ag(111) and Au(111). Therefore, formation of water domains would be energetically slightly favorable. On the other hand, since the energy difference is modest, which is particularly true for Ag, formation of the mixed O/O_2 and water structures would be formed eventually because of the entropy effect. As discussed later, OH group may form during CO oxidation with the presence of the water, and we expect that mixed water/OH structures may occur on Ag(111) and Au(111) surfaces, as found on Pt(111).[53]

In brief summary, the two types of interactions identified here, the H bondings and the interactions mediated through the substrates, exists in general once water molecules are involved. Similar phenomena have also been observed in much involved systems, for instance, on H_2O/O_2 on $TiO_2(110)$ surfaces by Liu and Hu[36] and H_2O/O_2 on free and supported gold clusters.[37] As discussed below, the strong interaction between water and reactants affects significantly on the CO oxidation.

5. Effect of H_2O on CO Oxidation

Having studied the promotion of adsorbed H_2O on the molecular adsorptions on metal surfaces, we are now in a position to address the effects of H_2O on the CO oxidation, specifically the effect of H_2O on the two possible routes (i) $O_2 \rightarrow 2O$, $CO + O \rightarrow CO_2$ and (ii) $CO + O_2 \rightarrow O_2\cdots CO \rightarrow CO_2 + O$. For the path (i), we only investigate the effect of H_2O on the O_2 dissociation, which was known as the rate limiting step for CO oxidation on Ag (111) and Au(111) surfaces. To simplify the discussion, we discuss here only the result of Ag(111). We expect that the conclusions obtained apply well on Au, which has been studied extensively in the literatures.[21−28]

We first investigated the effect of H_2O on the O_2 dissociation. Within a (2 × 2) unit cell, the two ends of O_2 molecules at the initial states with b-h-t configuration connects individually through a H bond to H atom in H_2O molecule on Ag(111) (see Figure 4b). Stretching O−O bond gradually, the transition state (Figure 6a) was approached at the O−O bond length of 1.92 Å. The O_2 dissociation barrier was calculated to be 0.96 eV, which is just 0.07 eV lower than that on clean Ag(111) (Figure 2). The effect of water looks modest in contrast to the significant stabilization of water on the adsorption of O_2 by 0.54 eV. To check the structures at TS of O_2 dissociation with (Figure 6a) and without (Figure 3a) the presence of water, we find that, with the presence of water, one atomic oxygen stays at energetically unfavorable atop site due to the constraint of the H bond formed with neighbor water molecules. The reason for

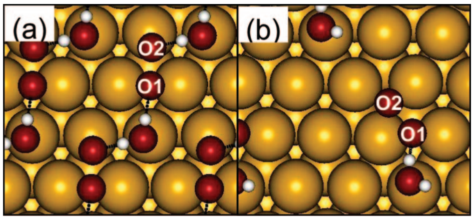

Figure 6. Schematic structures at the transition states for O_2 dissociation with the presence of H_2O on Ag(111) (2 × 2) (a) and (3 × 3) (b) unit cells.

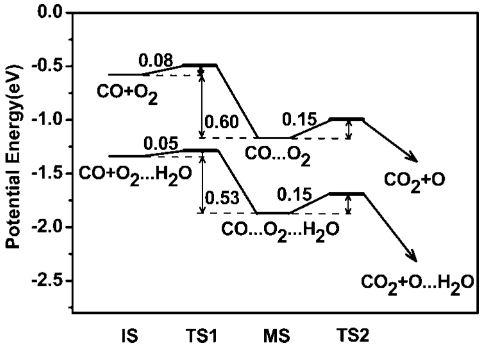

Figure 7. Potential energy surfaces for CO + O_2 → O_2···CO → CO_2 + O reaction without (top) and with (bottom) the presence of H_2O on the Ag(111) surface at initial state (IS), first transition state (TS1), metastable intermediate (MS), and the second transition state (TS2).

TABLE 6: Structural Parameters for the Calculated Initial States, the First Transition States (TS1), Meta Stable States (MS), and the Second Transition States, as Shown in Figure 8, for CO + O_2 → O_2···CO → CO_2 + O Reaction with the Presence of H_2O on Ag(111)[a]

	energy	d(O1−O2)	d(C−O2)	d(O1−H)	d(O−C−O1)
IS	$E_{coads} = -1.34$	1.45	2.50	1.99	108.0
TS1	$E_{act} = 0.05$	1.45	1.80	1.85	111.1
MS	$E_{coads} = -1.87$	1.47	1.35	1.89	118.8
TS2	$E_{act} = 0.15$	1.67	1.32	1.91	121.2

[a] The unit of length is angstroms and of energy is electronvolts.

this comes from the limited size of supercell used. The constraint can however be released if O_2 binds with water molecules via H bond only at one end and another end of O are free to relax. This was tested in a (3 × 3) unit cell, and the transition states located are shown in Figure 6b. Indeed, there is no unfavorable top site O anymore; instead it displaces to favorable hollow sites nearby. The transition state identified is similar to the TS of O_2 on clean Ag(111) (Figure 3a), except for the formation of a H bond with neighbor H_2O. Correspondingly, the TS is stabilized, and the calculated barrier is 0.67 eV, 0.36 eV lower than that of clean Ag(111) with barrier of 1.03 eV. The potential energy surface of O_2 dissociation with the presence of H_2O is shown in Figure 2. Though the barrier for O_2 dissociation decreases significantly with the presence of the water, it remains higher than the adsorption energy of the reactants. Namely, oxygen molecules still prefer to desorb, instead of the dissociation. Correspondingly, the activity for CO oxidation with dissociated atomic oxygen is low.

The effect of water on CO oxidation via the CO + O_2 → O_2···CO → CO_2 + O route was studied by placing CO and O_2 with H_2O in a Ag(111) (2 × 3) unit cell. We explored a number of possible high-symmetry sites and found that the CO on the top site near to the 1D zigzag O_2 and H_2O chain (Figure 4b) was energetically most favorable, as shown schematically in Figure 7. From this geometry, O_2 displaces toward CO, forming a four-center transition state (TS1 in Figure 7 and structural parameters given in Table 6) with barrier less than 0.05 eV. At TS1, the bond length between C and O2 in O_2 was 1.80 Å. After TS1, a meta-stable (MS) intermediate O_2···COcomplex with C−O2 bond length of 1.35 Å is formed, and the O_2 molecule with bond length of 1.47 Å rotates clockwise with molecular axis toward CO (Figure 7). Compared to the energy at IS ($E_{coads} = -1.34$ eV), the formation of the meta-stable state is an exothermic process with reaction energy of 0.53 eV, and corresponding potential energy surface is −1.87 eV. The O−O bond in the O_2···CO complex is stretched further, and the second transition state (TS2, Figure 7) with a barrier of 0.15 eV is reached when the O−O bond length is 1.67 Å. After TS2, CO_2 forms and desorbs from the surfaces, and one atomic oxygen (O1) is left and coadsorb with water molecules on the surfaces. The structures for IS, TS1, MS, and TS2 are shown schematically in Figure 8. For the whole reaction path, we find that there is always one or two H bonds that exist between O and H_2O, which stabilizes the system and lowers the overall energetics, correspondingly. For comparison, CO oxidation via O_2···CO complex without the presence of water was studied, and a calculated PES was plotted in Figure 7. Compared to the result with the presence of water, a similar energy profile was obtained, except a constant upshift of PES by ~0.7 eV due to the absence of the H bonds. The consequence for this overall upshift of PES is that the CO/O_2 interacts weakly with the substrates and may not stay on the surfaces for sufficient long time to allow reaction taking places, though CO oxidation via O_2 looks kinetically favorable even without the presence of water.

6. Discussions

For CO oxidation on Ag(111) and Au(111), the demanding activation for O_2 dissociation and weak adsorption of CO and O_2/O lead to very low activity on these two surfaces. The present work shows that the activity can however be enhanced significantly by addition of water in the system, because of the stabilization of the reactants and various intermediates by formation of the H bonds and/or the interaction mediated through the substrates. After formation of CO_2 via the the O_2···CO complex, one atomic oxygen is left and coadsorbed with water molecules on the surfaces. Since atomic oxygen can react readily with adsorbed CO (the barrier is 0.20 eV); free adsorption sites can accommodate additional O_2 and CO, and the catalytic cycle is closed. The overall barrier for the whole process is 0.20 eV only. In this reaction pathway, key points are highlighted as follows: (1) no demanding O_2 dissociation is required; instead, O_2 reacts with CO directly to form CO_2. (2) The promotion of water lies in the stabilization of various reactants/intermediates, and importantly water molecules do not involve directly in CO oxidation.

In this picture, the atomic oxygen formed after formation of CO_2 via the O_2···CO complex would react with additional CO to complete the catalytic cycle. However, the atomic oxygen may react with coadsorbed water to form hydroxyl groups, as found in recent experimental and theoretical studies.[35,54] Particularly, Mullins, Henkelman, and co-workers[35] found that the barrier for formation of hydroxyl groups from H_2O and atomic O on Au(111) was 0.11 eV. Moreover, they found that CO_2 was able to be formed readily (the barrier was less than 0.11 eV) by reaction between CO and hydroxyl groups via a concerted hydrogen transfer from one OH group to another, which stabilizes the transition state for CO oxidation. Ac-

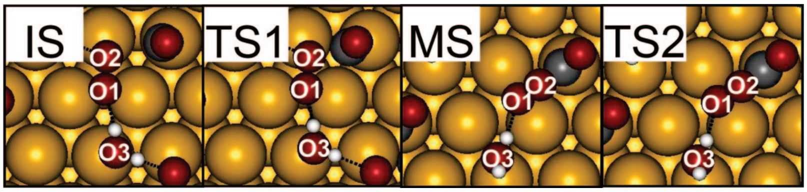

Figure 8. Schematic structures for IS, TS1, MS, and TS2 in Figure 7.

companied isotope experiments showed indeed that CO oxidation was promoted by water on atomic oxygen-covered Au(111), and direct participation of water molecules in the CO oxidation was identified unambiguously.

Mullins, Henkelman, and co-workers' findings[35] on direct involvement of water molecules in CO oxidation with hydroxyl group was interesting, because it provides additional reaction pathways for CO oxidation at low temperatures, besides the reaction pathway identified in the present work, where water molecules act as spectators to stabilize the various reactants and intermediates. In this context, we note that the formation of hydroxyls from water dissociation on clean Ag(111) and Au(111) surfaces are activated processes, and DFT calculations showed that the barrier for water dissociation on Au(111) is ~3.0 eV.[55] Formation of hydroxyls can, however, be promoted dramatically with preadsorbed atomic oxygen, as shown in ref 35. On the other hand, the barriers for O_2 dissociation on these two surfaces even with the presence of water are still considerably high, as shown by the present calculations. However, atomic oxygen can be generated eventually after CO oxidation with O_2 molecules assistant by coadsorbed water, as discussed above. Thus, atomic oxygen formed may either react with CO to form CO_2 directly or react with H_2O to form OH groups, which meet CO to form CO_2 sequentially. Both reaction pathways are kinetic competitive, and would increase the overall reaction rates for CO oxidation, correspondingly.

The hydroxyl group formed may interact with water molecules through the mechanism (H bonds and substrate mediated interactions) described in this work. The stabilization affects not only hydroxyls but also water molecules.[56,57] This may help to increase the coverage of water, and promotion of water on the CO oxidation would be enhanced further.

Though the effect of water on CO oxidation is focused on the metal surfaces in the present work, the mechanisms identified may have general effect on various reactions with water involved, as indeed reported in the literature.[33−37] For instance, Liu and Hu[36] investigated the effect of water in CO oxidation on $Au/TiO_2(110)$ using DFT. They found that water dissociates readily into OH groups, which stabilizes/facilitates O_2 adsorption and diffusion on TiO_2, necessary for following CO oxidation. Landman and co-workers showed that coadsorption of H_2O and O_2 on free or supported gold clusters leads to formation of a complex well bound to the gold cluster due to the synergic partial proton sharing between adsorbates.[37] The O−O bond is thus activated, leading to a small activation barrier for CO oxidation (0.5 eV).

7. Conclusions

In summary, we present here a systematic density functional theory study of the promotion of water on CO oxidation on Ag(111) and Au(111) surfaces. It is found that, though elementary reactions between CO and atomic oxygen are facile with modest barriers of 0.20 eV for Ag(111) and 0.29 eV for Au(111), considerable O_2 activation (1.03 eV for Ag(111) and 1.97 eV for Au(111)) and weak binding of reactants limit overall reactivity of these two surfaces for CO oxidations. Our calculations show that the presence of water stabilizes substantially the adsorption of reactants, such as O_2, atomic O, and CO, via formation of the H bonds and/or the interactions mediated through the substrates between the adsorbates, accordingly. Moreover, we find that adsorbed water molecules stabilize the transition states and various intermediates by similar interactions. The barrier for O_2 dissociation on Ag(111) becomes 0.67 eV (0.37 eV lower than clean surface) with the presence of water, which remains considerable. Adsorbed water molecules stabilizes the $O_2 \cdots CO$ complex, which leads to the formation of CO_2 and atomic oxygen via four center transition states with barrier of ~0.15 eV. Atomic oxygen formed may either react with adsorbed CO, or reacts with adsorbed water to form hydroxyls, which oxidizes CO subsequently, to complete the catalytic cycle.

Acknowledgment. We are thankful for the financial support from Natural Science Foundation of China (20503030, 20733008, 20573107) and Ministry of Science and Technology (2007CB815205).

References and Notes

(1) Ertl, G. *Surf. Sci.* **1994**, *299*, 742.
(2) Wintterlin, J.; Volkening, S.; Janssens, J. V. W.; Zambelli, T.; Ertl, G. *Science* **1997**, *278*, 1931.
(3) Valden, M.; Lai, X.; Goodman, D. W. *Science* **1998**, *281*, 1647.
(4) Eichler, A.; Hafner, J. *Phys. Rev. Lett.* **1997**, *79*, 4481.
(5) Dupont, C.; Jugnet, Y.; Loffreda, D. *J. Am. Chem. Soc.* **2006**, *128*, 9129.
(6) Gong, X. Q.; Liu, Z. P.; Raval, R.; Hu, P. *J. Am. Chem. Soc.* **2004**, *126*, 8.
(7) Kandoi, S.; Gokhale, A. A.; Grabow, L. C.; Dumesic, J. A.; Mavrikakis, M. *Catal. Lett.* **2004**, *93*, 93.
(8) Remediakis, I. N.; Lopez, N.; Nørskov, J. K. *Angew. Chem., Int. Ed.* **2005**, *44*, 1824.
(9) Huber, H.; McIntosh, D.; Ozin, G. A. *Inorg. Chem.* **1977**, *16*, 975.
(10) Wallace, W. T.; Whetten, R. L. *J. Am. Chem. Soc.* **2002**, *124*, 7499.
(11) Hagen, J.; Socaciu, L. D.; Elijazyfer, M. U. H.; Bernhardt, T. M.; Wöste, L. *Phys. Chem. Chem. Phys.* **2002**, *4*, 1707.
(12) Liu, Z. P.; Hu, P.; Alavi, A. *J. Am. Chem. Soc.* **2002**, *124*, 14770.
(13) Molina, L. M.; Hammer, B. *Phys. Rev. Lett.* **2003**, *90*, 206102.
(14) Burghaus, U.; Vattuone, L.; Gambardella, P.; Rocca, M. *Surf. Sci.* **1997**, *374*, 1.
(15) Burghaus, U.; Conrad, H. *Surf. Sci.* **1996**, *352−354*, 253.
(16) Burghaus, U.; Conrad, H. *Surf. Sci.* **1996**, *364*, 109.
(17) Burghaus, U.; Conrad, H. *Surf. Sci.* **1997**, *374*, 1.
(18) Barth, J. V.; Zambelli, T. *Surf. Sci.* **2002**, *513*, 359.
(19) Paker, D. H.; Koel, B. E. *J. Vac. Sci. Technol. A* **1990**, *8*, 2585.
(20) Bondzie, V. A.; Parker, S. C.; Campbell, C. T. *J. Vac. Sci. Technol. A* **1999**, *17*, 1717.
(21) Schubert, M. M.; Hackenberg, S.; van Veen, A. C.; Muhler, M.; Plzak, V.; Behm, R. J. *J. Catal.* **2001**, *197*, 113.
(22) Grisel, R. J. H.; Nieuwenhuys, B. E. *J. Catal.* **2001**, *199*, 48.
(23) Sanchez, A.; Abbet, S.; Heiz, U.; Schneider, W.-D.; Hakkinen, H.; Barnett, R. N.; Landman, U. *J. Phys. Chem. A* **1999**, *103*, 9573.
(24) Haruta, M. *Catal. Today* **1997**, *36*, 153.
(25) Haruta, M.; Tsubota, S.; Kobayashi, T.; Kageyama, H.; Genet, M. J.; Delmon, B. *J. Catal.* **1993**, *144*, 175.
(26) Bollinger, M. A.; Vannice, M. A. *Appl. Catal. B* **1996**, *8*, 417.
(27) Tsubota, S.; Nakamura, K.; Tanaka, K.; Haruta, M. *Catal. Lett.* **1998**, *56*, 131.
(28) Kozlov, A. I.; Kozlova, A. P.; Liu, H.; Iwasawa, Y. *Appl. Catal. A* **1999**, *182*, 9.

(29) Stiehl, J. D.; Kim, T. S.; McClure, S. M.; Mullins, C. B. *J. Am. Chem. Soc.* **2004**, *126*, 13574.

(30) Date, M.; Haruta, M. *J. Catal.* **2001**, *201*, 221.

(31) Bergeld, J.; Kasemo, B.; Chakarov, D. V. *Surf. Sci.* **2001**, *495*, L815.

(32) Gong, X. Q.; Hu, P.; Raval, R. *J. Chem. Phys.* **2003**, *119*, 6325.

(33) Date, M.; Okumura, M.; Tsubota, S.; Haruta, M. *Angew. Chem., Int. Ed.* **2004**, *43*, 2129.

(34) Kim, T. S.; Gong, J. L.; Ojifinni, R. A.; White, J. M.; Mullins, C. B. *J. Am. Chem. Soc.* **2006**, *128*, 6282.

(35) Ojifinni, R. A.; Froemming, N. S.; Gong, J. L.; Pan, M.; Kim, T. S.; White, J. M.; Henkelman, G.; Mullins, C. B. *J. Am. Chem. Soc.* **2008**, *130*, 6801.

(36) Liu, L. M.; McAllister, B.; Ye, H. Q.; Hu, P. *J. Am. Chem. Soc.* **2006**, *128*, 4017.

(37) Bongiorno, A.; Landman, U. *Phys. Rev. Lett.* **2005**, *95*, 106102.

(38) Hammer, B.; Hansen, L. B.; Nørskov, J. K. *Phys. Rev. B* **1999**, *59*, 7413.

(39) Perdew, J. P.; Chevary, J. A.; Vosko, S. H.; Jackson, K. A.; Pederson, M. R.; Singh, D. J.; Fiolhais, C. *Phys. Rev. B* **1992**, *46*, 6671.

(40) White, J. A.; Bird, D. M. *Phys. Rev. B* **1994**, *50*, 4954.

(41) Chase, M. W. *JANAF Thermochemical Tables*, 3rd ed.; American Chemical Society and American Institute of Physics for the National Bureau of Standards: Washington, DC, 1986.

(42) Mavrikakis, M.; Stoltze, P.; Norskov, J. K. *Catal. Lett.* **2000**, *64*, 101.

(43) Montoya, A.; Haynes, B. S. *J. Phys. Chem. C* **2007**, *111*, 1333.

(44) *NIST Computational Chemistry Comparison and Benchmark Database*, NIST Standard Reference Database Number 101; Release 10 ed.; Johnson, R. D., III, Ed., 2004.

(45) Su, H. Y.; Bao, X. H.; Li, W. X. *J. Chem. Phys.* **2008**, *128*, 194707.

(46) Xu, Y.; Greeley, J.; Mavrikakis, M. *J. Am. Chem. Soc.* **2005**, *127*, 12823.

(47) Blyholder, G. *J. Phys. Chem.* **1964**, *68*, 2772.

(48) Buatier de Mongeot, F.; Valbusa, U.; Rocca, M. *Surf. Sci.* **1995**, *339*, 291.

(49) Linsmeier, Ch.; Wanner, J. *Surf. Sci.* **2000**, *454−456*, 305.

(50) Yang, M. M.; Bao, X. H.; Li, W. X. *J. Phys. Chem. C* **2007**, *111*, 7403.

(51) Michaelides, A.; Morgenstern, K. *Nat. Mater.* **2007**, *6*, 597.

(52) Meng, S.; Wang, E. G.; Gao, S. W. *Phys. Rev. B* **2004**, *69*, 195404.

(53) Clay, C.; Haq, S.; Hodgson, A. *Phys. Rev. Lett.* **2004**, *92*, 046102.

(54) Wang, G.-C.; Tao, S.-X.; Bu, X.-H. *J. Catal.* **2006**, *244*, 10.

(55) Rodriguez, J. A.; Ma, S.; Liu, P.; Hrbek, J.; Evans, J.; Pérez, M. *Science* **2007**, *318*, 1757.

(56) Yamamoto, S.; ersson, K.; Bluhm, H.; Ketteler, G.; Starr, D. E.; Schiros, T.; Ogasawara, H.; Pettersson, L. G. M.; Salmeron, M.; Nilsson, A. *J. Phys. Chem. C* **2007**, *111*, 7848.

(57) Andersson, K.; Ketteler, G.; Bluhm, H.; Yamamoto, S.; Ogasawara, H.; Pettersson, L. G. M.; Salmeron, M.; Nilsson, A. *J. Am. Chem. Soc.* **2008**, *130*, 2793.

JP803400P